

## Semiconductor Surface Roughness: Dependence on Sign and Magnitude of Bulk Strain

Y. H. Xie,<sup>1</sup> G. H. Gilmer,<sup>1</sup> C. Roland,<sup>2</sup> P. J. Silverman,<sup>1</sup> S. K. Buratto,<sup>1</sup> J. Y. Cheng,<sup>1</sup> E. A. Fitzgerald,<sup>1</sup> A. R. Kortan,<sup>1</sup> S. Schuppler,<sup>1</sup> M. A. Marcus,<sup>1</sup> and P. H. Citrin<sup>1</sup>

<sup>1</sup>AT&T Bell Laboratories, Murray Hill, New Jersey 07974

<sup>2</sup>Department of Physics, North Carolina State University, Raleigh, North Carolina 27695

(Received 20 June 1994)

Changes in surface roughness have been studied as a function of bulk compressive and tensile strains (biaxial in the plane of the sample surface) in thin films of compositionally uniform and dislocation-free  $\text{Ge}_{0.5}\text{Si}_{0.5}$ . A pronounced surface roughness is observed only for films under compressive strains exceeding 1.4%. Molecular dynamics simulations show that this striking result has its origin in the strain-induced lowering of surface step free energies.

PACS numbers: 68.35.Bs

It is well established that bulk strain plays an important role in determining the structure of semiconductor surfaces [1–3]. For example, an undulated surface has larger surface area and thus higher surface free energy, which is counterbalanced by the reduction in strain energy near the surface. Previous work has treated the surface as a continuum, neglecting details of reconstruction and the presence of steps [4–7]. Strictly speaking, a continuum model is valid only above the roughening transition temperature [8], but in the case of the Si(100) surface, there is no evidence for roughening transitions below the melting temperature of bulk Si. Equally important, such a simplified treatment of the surface necessarily ignores the *sign* of the underlying bulk strain, i.e., whether the strain is tensile or compressive [4–7].

Here, we report a startling effect of strain on the roughness of a semiconductor surface: The surface is flat under tension but rough under compression. Based on molecular dynamics simulations, we show that this behavior is traceable to the structure of different surface steps and their response to different types of strain. Our results, although specific to the system studied, demonstrate in general that consideration of surface step free energies is essential for reliably describing semiconductor surface morphologies.

A unique feature of this work is that the same semiconductor is studied while only varying the underlying bulk strain. This is accomplished through the novel use of random alloy  $\text{Ge}_{0.5}\text{Si}_{0.5}$  films grown on relaxed, compositionally graded  $\text{Ge}_x\text{Si}_{1-x}$  buffer layers, see Fig. 1. The buffer layers are epitaxially deposited on Si(100) substrates (of less than  $\pm 0.5^\circ$  misorientation) with a linearly graded Ge concentration rate of 10% Ge/ $\mu\text{m}$ , and capped with a  $1\ \mu\text{m}$  thick layer of uniform composition [9]. The root-mean-square (RMS) roughness of the cap layer surface before growing the  $\text{Ge}_{0.5}\text{Si}_{0.5}$  film is  $< 5\ \text{\AA}$ . It is the final Ge content in this cap layer,  $x_f$  in  $\text{Ge}_{x_f}\text{Si}_{1-x_f}$  that determines the magnitude and sign of the strain induced in the overlying  $50\ \text{\AA}$  thick  $\text{Ge}_{0.5}\text{Si}_{0.5}$  films.

Starting with pure Si ( $x = 0$ ), the  $\text{Ge}_x\text{Si}_{1-x}$  buffer layers were grown at  $900^\circ\text{C}$ . The temperature was then scaled down in proportion to the decreasing melting points of subsequently grown material. This procedure resulted in essentially strain-free layers containing threading dislocation densities  $< 5 \times 10^6\ \text{cm}^{-2}$  [10]. The lattice constant at the surface of these relaxed buffer layers was determined by x-ray diffraction measurements in a  $\vartheta$ - $2\vartheta$  configuration, where  $\vartheta$  relates directly to the out-of-plane lattice constant.

The  $\text{Ge}_{0.5}\text{Si}_{0.5}$  films were grown on the different cap layers under conditions of constant composition, thickness, growth rate ( $1\ \text{\AA}/\text{sec}$ ), and growth temperature ( $650^\circ\text{C}$ ). This procedure and choice of parameters [11] ensured that the morphologies of the films were domi-

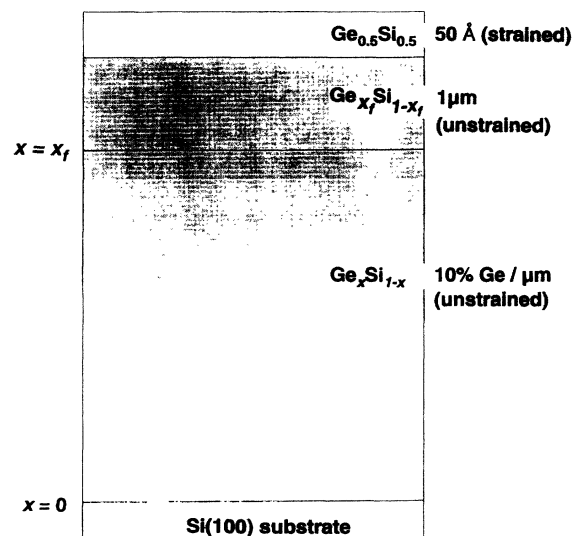


FIG. 1. Schematic view of a generic sample structure (actual linear grading in  $\text{Ge}_x\text{Si}_{1-x}$  buffer layers is much more gradual than shown). Strain in the upper  $\text{Ge}_{0.5}\text{Si}_{0.5}$  film can be changed from 2% tensile to 2% compressive by varying the final value of  $x$ ,  $x_f$ , between 1 and 0 (when  $x_f = 1$ , a Ge(100) substrate is used).

nated by surface energetics rather than kinetics. The uniformity, i.e., randomness, of the films was determined by extended x-ray absorption fine structure (EXAFS) [12] measurements of the Si and Ge nearest-neighbor environments in the two most extreme cases, a  $\text{Ge}_{0.5}\text{Si}_{0.5}$  film grown on a pure Ge(100) and a pure Si(100) substrate. The corresponding Si  $K$ - and Ge  $K$ -edge data [13] showed average Si and Ge first-shell coordination fractions of  $0.50 \pm 0.03$  in both samples, indicating the absence of any significant phase segregation or clustering. Planview and cross-sectional transmission electron (TEM and XTEM) microscopies were used to look for dislocations in the films. The only ones detected over the entire range of samples were scattered  $90^\circ$  partials in the smoothest sample [14], nucleated from large particles with densities too low to affect the strain in the alloy films.

The  $\text{Ge}_{0.5}\text{Si}_{0.5}$  films experienced strains ranging from 2% tensile on a 100% Ge substrate to 2% compressive on a 0% Ge (i.e., Si) substrate. Intermediate strain values were deduced from the x-ray diffraction values of the relaxed buffer layer surface lattice constants. Measurements of surface roughness were obtained using atomic force microscopy (AFM) [15]. Figure 2 shows AFM micrographs for several representative films under different types and amounts of strain. Substantial surface roughness is apparent for the film under 2% compression, while no detectable roughness is observed for films under tensile strains of up to 2%. Fourier analysis of the AFM data shows no obvious change in spatial wavelength for

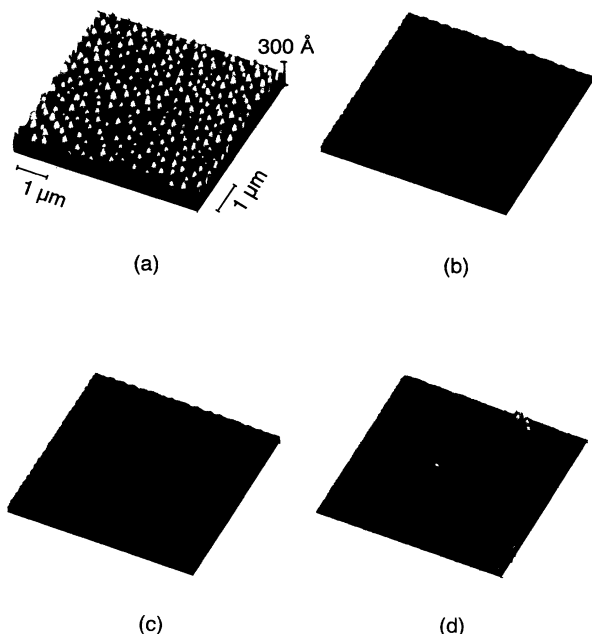


FIG. 2. Atomic force micrographs of  $\text{Ge}_{0.5}\text{Si}_{0.5}$  films under (a) 2% compressive, (b) 1% compressive, (c) 0.5% compressive, and (d) 2% tensile strains. Scattered protrusions in (d) are particulates on sample surface. Dimensions shown in (a) apply to all micrographs.

any of the films exhibiting roughness. The degree of surface roughness is quantified and plotted as a function of strain in Fig. 3. The results are striking.

The TEM and EXAFS data from these films definitively rule out misfit dislocations [16] and phase segregation as possible explanations for the observed roughening. The fact that only the substrates are varied while keeping the growth conditions and stoichiometry of the alloy films constant precludes still other artifactual explanations related to film growth kinetics and composition. Indeed, the possibility that these results apply only to alloy films can be eliminated based on our additional studies of a  $50 \text{ \AA}$  thick pure Si film growth on relaxed  $\text{Ge}_{0.3}\text{Si}_{0.7}$  (i.e., under tension) and a  $50 \text{ \AA}$  thick pure Ge film grown on relaxed  $\text{Ge}_{0.7}\text{Si}_{0.3}$  (i.e., under compression). Only in the latter case was a rough surface observed, confirming that strain is the dominant factor responsible for the differences in surface morphology [17]. Moreover, we find again that the sign of the strain is decidedly important.

Since a rough surface implies a high density of steps, we must consider the role of step formation on the (100) surface under different conditions of strain. There are different step structures formed on this surface which have been studied extensively [18], and only a few relevant features require mentioning here. A vicinal Si(100) or Ge(100) surface consists of flat terraces of dimer bonds separated by single- or double-height steps. At small miscut angles, and when the terraces are separated by single-height steps, the dimerization necessarily alternates between geometries of  $(2 \times 1)$  and  $(1 \times 2)$  surface reconstruction. A single-height step is denoted  $S_A$ , when the dimer bonds on the upper terrace are perpendicular to the step edge and  $S_B$  when they are parallel, see Fig. 4. Unlike the single-height steps, the corresponding double-height steps, denoted  $D_A$  and  $D_B$ , need not come in pairs since a dimer rotation is not involved [19].

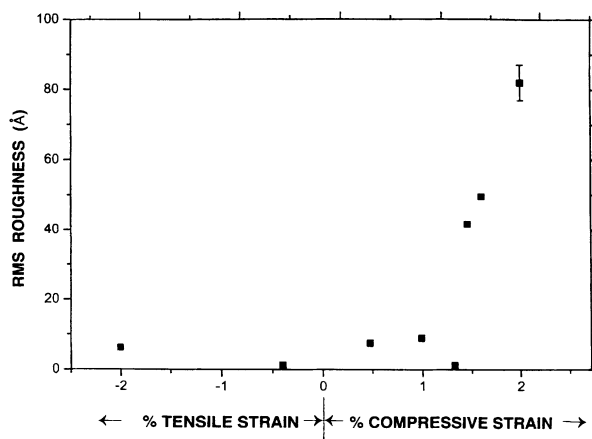


FIG. 3. Root-mean-square surface roughness derived from atomic force microscopy data versus strain.

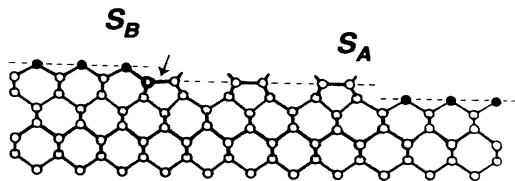


FIG. 4. Schematic side view of  $S_A$  and  $S_B$  single-height steps on the (100) surface of Si or Ge. A [110] projection is shown. Dimer bonds on the  $(2 \times 1)$  terrace are horizontal, while those on the  $(1 \times 2)$  terrace (normal to the plane of the figure) are shown as solid circles. Those dimer bonds under higher tensile strain are indicated by the arrow.

At the heart of characterizing step formation is the step free energy, defined as the free energy difference between a surface with and without a step. We gain insight into the behavior of step free energies as a function of film strain by using molecular dynamics simulations with the Stillinger and Weber potential [20]. This empirical potential reproduces many of the features of the Si(100) surface and has been successfully applied to the study of step energy variations with terrace widths [21]. However, since this model is also known to underestimate the surface energy of real Si, we focus our attention on the relative change in step energies with varying film strains rather than on the absolute values.

The simulations were carried out here as in a previous study [21], and we use the same notation. Slabs of the properly dimerized, stepped structure were constructed (the computational cell contains two ledges with periodic boundary condition), put under a given strain, then relaxed at zero temperature (at which the step free energy is identical with the step energy). Large systems (more than 60 atomic layers thick) were considered, thereby ensuring proper strain relaxation in the bulk crystal. The total energy of the structure  $E$  was calculated, and then the step energy per ledge atom  $\lambda$  was determined from  $\lambda = (E - N\varepsilon_b - L_x L_y \varepsilon_s) / N_l$ . Here,  $N$  and  $N_l$  are the total number of atoms in the slab and in the ledge, and  $L_x$  and  $L_y$  are the horizontal lengths. The bulk and surface energies of the crystal,  $\varepsilon_b$  and  $\varepsilon_s$ , depend sensitively upon the strain and were determined in separate calculations.

In Fig. 5 we plot the step energies for the  $S_B$  and  $D_B$  steps as a function of terrace width on a Si(100) surface under 2% tensile, 2% compressive, and zero strain. The overall trends of the step energy with terrace width follow the predictions of standard continuum theory [22,23]. The new insight provided here, which cannot be addressed by continuum theory, is how the step energy—and thus the surface roughness—varies with the sign of the strain: Compressive strain lowers the step energy, thereby promoting surface roughening, while tensile strain raises the step energy, thereby inhibiting it. Note that the differences between the strained and unstrained  $S_B$  (and  $D_B$ ) step energies are quite high. At a 2% compressive strain, for example, these energy differences are as large

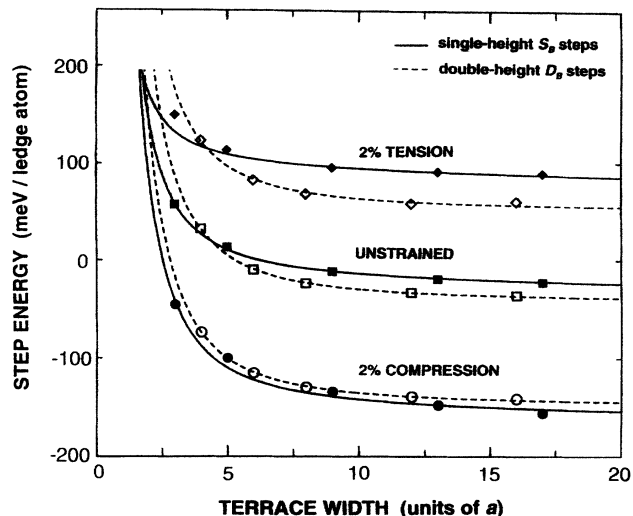


FIG. 5. Step energy per ledge atom versus terrace width for  $S_B$  steps (solid lines) and  $D_B$  steps (dashed lines) on a Si(100) surface under three different conditions of strain. The terrace width is in units of  $a = a_0/\sqrt{2} = 3.84 \text{ \AA}$ . The absolute step energy values are not accurate but the relative shifts due to strain are.

as 150 meV/ledge atom. By contrast, our calculations show that the effects of strain on the step energies of  $S_A$  steps are very much smaller ( $<5$  meV/ledge atom) and were not included in Fig. 5.

The origin of the different effects of strain on the  $S_A$  and  $S_B$  steps lies in the special row of dimer bonds located along the base of the  $S_B$  step edges [24], indicated by the arrow in Fig. 4. Unlike all the other surface dimer bonds involving “nonbonded” atoms (i.e., with a dangling bond) that lie within the flat  $(2 \times 1)$  or  $(1 \times 2)$  terraces, these special dimer bonds involve a row of “bonded” atoms that are part of the  $S_B$  step itself and are therefore much more rigid. There is a correspondingly greater tensile strain on these dimer bonds, explaining why the  $S_B$  step energy is higher (44 meV/ledge atom) than that of the  $S_A$  step in an unstrained surface. Now, placing the film under compression has the predictable effect of relieving this inherent  $S_B$ -step-induced tensile strain and thus significantly reducing the  $S_B$  step energy. Conversely, placing the film under an additional tensile strain serves to increase the  $S_B$  step energy. It follows that the  $S_A$  step energy, which is already lower because of the absence of these special dimer bonds, remains essentially unaffected by strains of either sign.

Surface undulation can, in principle, involve steps of only single height, only double height, or a combination of the two. Since both  $S_A$  and  $S_B$  steps must be present for an undulated surface of just single-height steps, the one with higher step energy  $S_B$  becomes the limiting factor for the undulation to develop. An undulated surface of only double-height steps has no analogous topological requirements, so the much higher step energy for  $D_A$  (238 meV/ledge atom) means that

only the  $D_B$  step energy need be considered. Our results showing the effects of strain on only the  $S_B$  and  $D_B$  step energies in Fig. 5 are therefore appropriate for describing the dominant factors controlling the development of undulations of this surface.

A general trend observed for all types of single and double steps is that step free energies decrease with increasing terrace width and eventually become negative. Thus, as had been predicted [23], a surface with steps is inherently more stable than one that is flat. Our findings here of compressive strain lowering the step energies of the roughness-limiting  $S_B$  and  $D_B$  steps implies that much smaller terrace widths, and thus higher step densities, become energetically favorable relative to the case of an unstrained surface. In competition with the surface energetics of an idealized surface, however, is the surface kinetics of a real one. It is well known that surface undulations with long spatial wavelength  $\Lambda$  approach but never reach their minimum energy configuration due to the  $\Lambda^4$  dependence of the time constant for the growth of the undulations' amplitude [25], as dictated by the mass transport on surfaces. The  $\leq 2\%$  strain is not expected to affect this behavior significantly. We speculate that it is this kinetic limitation which is responsible for the observation (see Fig. 3) of surface roughness in our films, starting at  $\sim 1.4\%$  compressive strain rather than at the idealized value of 0%.

In summary, we have studied the surface morphologies of thin  $\text{Ge}_{0.5}\text{Si}_{0.5}$  films under strains ranging from 2% compressive to 2% tensile. A marked increase in surface roughness is observed only for the cases of compressive strains larger than  $\sim 1.4\%$ . Care was taken to rule out misfit dislocations and phase segregation as possible alternate explanations for the roughness. Molecular dynamics simulations show that the reduction of step free energies under compressive strain is responsible for the observed surface roughening.

The x-ray absorption measurements were performed at the National Synchrotron Light Source, Brookhaven National Laboratory, which is supported by the DOE, Department of Materials Science and Division of Chemical Sciences.

- 
- [1] Y. W. Mo, D. E. Savage, B. S. Swartzentruber, and M. G. Lagally, *Phys. Rev. Lett.* **65**, 1020 (1990).
  - [2] D. J. Eaglesham and M. Cerullo, *Phys. Rev. Lett.* **64**, 1943 (1990).
  - [3] A. Sakai and T. Tatsumi, *Phys. Rev. Lett.* **71**, 4007 (1993).
  - [4] A. J. Pidduck, D. J. Robbins, and A. G. Cullis, *Inst. Phys. Conf. Ser.* **134**, 609 (1993).
  - [5] B. J. Spencer, P. W. Voorhees, and S. H. Davis, *Phys. Rev. Lett.* **67**, 3696 (1991).
  - [6] M. A. Grinfeld, *Sov. Phys. Dokl.* **31**, 831 (1987).
  - [7] D. J. Srolovitz, *Acta. Metall.* **37**, 621 (1989).

- [8] H. J. Leamy, G. H. Gilmer, and K. A. Jackson, in *Surface Physics of Materials*, edited by J. M. Blakely (Academic Press, New York, 1975).
- [9] Y. H. Xie, E. A. Fitzgerald, C. Monroe, P. J. Silverman, and G. P. Watson, *J. Appl. Phys.* **73**, 8364 (1993). A Ge(100) substrate was used when growing pure Ge buffer layers (i.e.,  $x = 1$ ).
- [10] E. A. Fitzgerald, Y. H. Xie, D. Monroe, P. J. Silverman, J. M. Kuo, A. R. Kortan, F. A. Thiel, and B. E. Weir, *J. Vac. Sci. Technol. B* **10**, 1807 (1992).
- [11] The film thickness of 50 Å is near the equilibrium critical layer thickness for no dislocations, cf., J. W. Matthews and A. E. Blakeslee, *J. Cryst. Growth* **27**, 118 (1974). The film growth temperature was established from experiments on the sample with the roughest surface (on a pure Si(100) substrate), where roughness and especially the Fourier components of the spatial wavelength varied dramatically for temperatures  $< 650^\circ\text{C}$ , but were unchanged at or above that temperature.
- [12] P. A. Lee, P. H. Citrin, B. M. Kincaid, and P. Eisenberger, *Rev. Mod. Phys.* **53**, 769 (1981).
- [13] The Si  $K\alpha$  and Ge  $K\alpha$  fluorescence yield EXAFS data were obtained with InSb(111) and Si(220) monochromating crystals using the AT&T Bell Laboratories X15B beamline at the National Synchrotron Light Source.
- [14] The separation of the  $90^\circ$  and  $30^\circ$  partials from a  $60^\circ$  complete dislocation under tensile strain has been well studied, cf., R. Hull, J. C. Bean, L. J. Peticolas, D. Bahnck, B. E. Weir, and L. C. Feldman, *Appl. Phys. Lett.* **61**, 2802 (1992); W. Wegscheider, K. Eberl, U. Menczgar, and G. Abstreiter, *Appl. Phys. Lett.* **57**, 875 (1990).
- [15] The AFM measurements used a Park Scientific Instrument AFM-BD2 scanning force microscope with conventional  $\text{SiN}_x$  pyramidal tips of  $70^\circ$  side wall profile and 400 Å tip radius. All images were taken in contact mode.
- [16] Interestingly, no dislocations were observed even in the roughest surface containing three-dimensional islands of  $\sim 300$  Å height. We attribute this to the increased dislocation nucleation barrier resulting from outward relaxation of the sidewalls in these islands, cf., A. G. Cullis, D. J. Robbins, A. J. Pidduck, and P. W. Smith, *J. Cryst. Growth* **123**, 333 (1992).
- [17] We have also studied alloy films ( $\text{Ge}_x\text{Si}_{1-x}$  with  $x < 0.5$  on Ge) under tensile strains  $> 2\%$ . These exhibit roughness, but (unlike the films with  $x = 0.5$ ) they also contain a high density of dislocations, making it difficult to isolate the source of the roughness.
- [18] For a good review, see J. E. Griffith, and G. P. Kochanski, *CRC Rev. Solid State Mater. Sci.* **16**, 255 (1990).
- [19] D. J. Chadi, *Phys. Rev. Lett.* **59**, 1691 (1987).
- [20] F. Stillinger and T. Weber, *Phys. Rev. B* **31**, 5262 (1985).
- [21] T. W. Poon, S. Yip, P. S. Ho, and F. Abraham, *Phys. Rev. Lett.* **65**, 2161 (1991); *Phys. Rev. B* **45**, 3521 (1992).
- [22] E. Pehlke and J. Tersoff, *Phys. Rev. Lett.* **67**, 465 (1991); *ibid.*, 1290 (1991).
- [23] O. L. Alerhand, D. Vanderbilt, R. Meade, and J. D. Joannopoulos, *Phys. Rev. Lett.* **61**, 1973 (1988).
- [24] Configurations involving nonbonded atoms at the base of the  $S_B$  step edge are not considered because of their much higher energies (see Ref. [21]).
- [25] W. W. Mullins, *J. Appl. Phys.* **30**, 77 (1959).

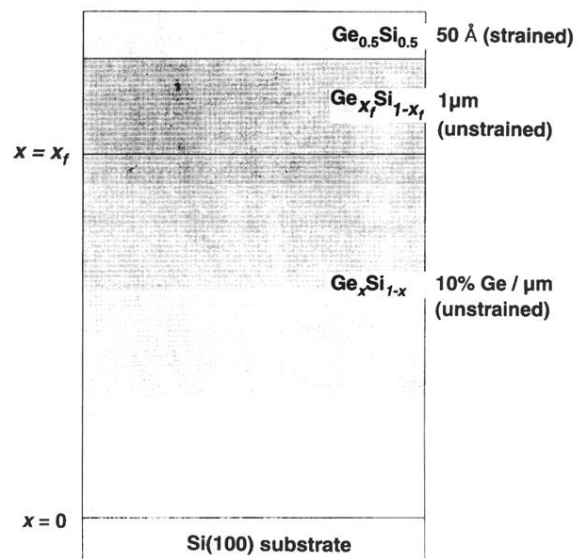


FIG. 1. Schematic view of a generic sample structure (actual linear grading in  $\text{Ge}_x\text{Si}_{1-x}$  buffer layers is much more gradual than shown). Strain in the upper  $\text{Ge}_{0.5}\text{Si}_{0.5}$  film can be changed from 2% tensile to 2% compressive by varying the final value of  $x$ ,  $x_f$ , between 1 and 0 (when  $x_f = 1$ , a Ge(100) substrate is used).

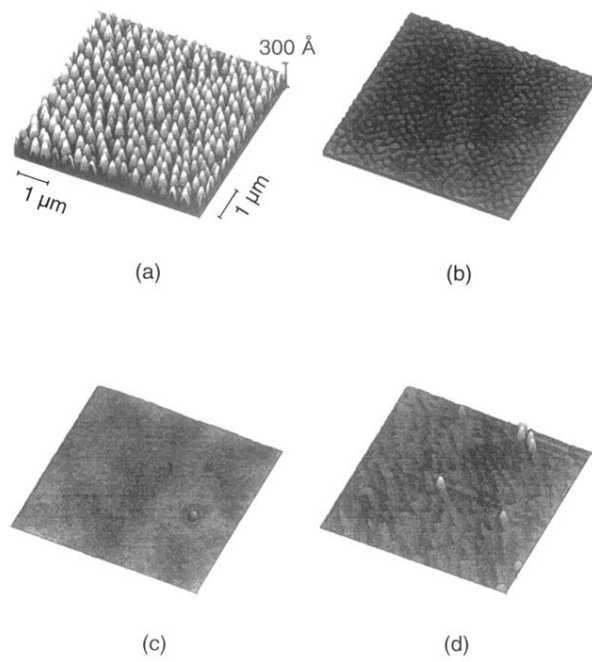


FIG. 2. Atomic force micrographs of  $\text{Ge}_{0.5}\text{Si}_{0.5}$  films under (a) 2% compressive, (b) 1% compressive, (c) 0.5% compressive, and (d) 2% tensile strains. Scattered protrusions in (d) are particulates on sample surface. Dimensions shown in (a) apply to all micrographs.